

Cluster AgeS Experiment: The Age and Distance of the Globular Cluster ω Centauri Determined from Observations of the Eclipsing Binary OGLEGC17

I. B. Thompson^{1,2}, J. Kaluzny^{2,3}, W. Pych³, G. Burley¹, W. Krzeminski⁴, B. Paczynski⁵,
S. E. Persson¹, and G. W. Preston¹

ABSTRACT

We use masses, radii, and luminosities of the detached eclipsing binary OGLEGC17 derived from photometric and spectroscopic observations to calculate the age and distance of the globular cluster ω Cen. Age versus turnoff mass and age versus luminosity relations from Girardi et al. (2000) yield two independent estimates of the age, $9.1 < t < 16.7$ Gyr and $12.9 < t < 18.5$ Gyr. The distance and distance modulus derived by use of the infrared versus surface brightness relation are $d = 5385 \pm 300$ pc and $(m - M)_V = 14.06 \pm 0.11$. Distances derived from our infrared surface brightness versus color relation and the T_{eff} versus $B - V$ color relation of Sekiguchi & Fukugita (2000) disagree by about 10 per cent. Major improvements in the accuracy in estimated age and distance can be made with better measurements of the masses of the components of OGLEGC17.

Subject headings: clusters: globular, distances, ages; binary stars: eclipsing

1. Introduction

Reconciliation of globular cluster ages and the Hubble time is a primary issue of contemporary observational astronomy. Heretofore, the single largest uncertainty in the calculation of globular cluster ages from color-magnitude diagram (CMD) data has been the distance error (Renzini 1991; VandenBerg, Bolte, and Stetson 1996), followed by the stellar model uncertainties associated with the choice of the mixing length parameter. The hopes that Hipparcos (Perryman et al. 1997) would resolve the distance issue have not been fulfilled. For example, recent determinations of the distance modulus to 47 Tuc based on Hipparcos subdwarfs gave a value of 13.57 (Reid 1998), while

¹Carnegie Observatories, 813 Santa Barbara St., Pasadena, CA 91101-1292

²Visiting Astronomer, Cerro Tololo Inter-American Observatory. CTIO is operated by AURA, Inc. under contract to the National Science Foundation.

³Copernicus Astronomical Center, Bartycka 18, 00-716 Warsaw, Poland

⁴Las Campanas Observatory, Casilla 601, La Serena, Chile

⁵Princeton University Observatory, Department of Astrophysics, 124 Peyton Hall, Princeton, NJ 08554-1001

the value based on Hipparcos red clump giants is 13.32 (Kaluzny et al. 1998). The most likely reason for the discrepancy is the comparison of nearby stars with distant stars, with imperfect understanding of the population effects.

We avoid these difficulties by measurements of stellar masses and radii in the eclipsing binary OGLEGC17 in the globular cluster ω Cen. Detached eclipsing double line spectroscopic binaries offer the opportunity to calculate age directly from age - turnoff mass predictions from stellar evolution models. Distance follows from a geometrical calculation that employs the Barnes-Evans relation (Barnes and Evans 1976) between color and surface brightness. The method is very simple, and is well described by Lacy (1977), who has used the method to measure the distances to a number of well studied systems (Lacy 1979). His distance determinations agree well with the recent trigonometric parallaxes obtained by Hipparcos (Semiñuk 2000). Stebbins (1910) was fully aware of the equivalent method to determine the surface brightness of the components of Algol, for which a trigonometric parallax had just been measured. A complete list of historical references can be found in Kruszewski and Semiñuk (1999).

There has been steady progress in the last few years in the empirical calibration of the Barnes-Evans relation with the direct determinations of angular diameters of many stars obtained with optical interferometers (Di Benedetto 1998), and there are excellent prospects of further improvement (Hajian et al. 1998). Until recently the only missing elements have been the detached eclipsing binaries in globular clusters. Recent massive photometric searches for the rare photometric signatures of gravitational microlensing have led to the discovery of over 10^5 new variable stars. In particular, the first detached eclipsing binary near a main sequence turnoff was found in the globular cluster ω Cen as a ‘secondary’ project of OGLE (Kaluzny et al. 1996). By now several more such systems have been found in several other globular clusters by our group.

Demonstrations of the practical power of using eclipsing binaries for distance determinations to the Large Magellanic Cloud have been recently presented by Bell et al. (1993) (HV 5936), Guinan et al. (1998) (HV 2274) and Fitzpatrick et al. (2000) (HV 982).

Detached binaries can also free us from problems associated with the mixing length parameter, because binaries can yield the mass-luminosity relation, and this is not affected by the mixing length parameter (Paczynski (1997) and references therein). Also, the helium abundance can be deduced if the two components are sufficiently different in mass. This is all possible because detached components are just two single stars, never affected by the complications of mass exchange, and their internal structure is not disturbed by the fact that they orbit each other. A practical demonstration that all stellar parameters can be determined with a high accuracy, given accurate photometry and spectroscopy, is provided by the catalog of well studied detached eclipsing binaries covering the spectral range from O to M (Anderson 1991).

In this paper we present observations of the detached eclipsing binary OGLEGC17 in the globular cluster ω Centauri (Kaluzny et al. 1996). This star has a period of 2.467 days. Eclipse depths are $\Delta V = 0.30$ and $\Delta V = 0.26$ for the primary and secondary eclipses, respectively. With

an observed color of $B - V = 0.64$ and an observed magnitude of $V = 17.16$ (out of eclipse), this system lies slightly above the top of the main sequence in the cluster color-magnitude diagram, consistent with the individual members of the binary being stars at or near the cluster turnoff. These parameters along with the shape of the light curve suggest that the system is completely detached, making it ideal to study. These observations are used to derive preliminary estimates of the masses of the constituent stars and the distance and age of the cluster.

In the next section we present a description of the observations and the reduction analysis. Following that we derive the age and distance of the cluster.

2. Observations

2.1. Optical Photometry

B , V and I light curves were obtained with the $2K \times 2K$ pixel TEK#5 CCD camera on the du Pont 2.5-m telescope at Las Campanas Observatory during the period April 21, 1995 through June 4, 1995. The field of view was 8.9×8.9 arcmin with scale of 0.26 arcsec/pixel. The individual frames were processed with IRAF⁶ software, and the photometry was measured with DoPhot (Schechter, Mateo, and Saha 1993). Several standard fields from Landolt (1992) were observed on 4 nights during the 1995 run. These observations were used to establish a transformation between the instrumental bvi and the standard BVI system. Unfortunately, the only night on which we observed Landolt standards along with OGLEGC17 turned out to be non-photometric. The zero points of our photometry of OGLEGC17 were established based on data collected during the 1997 observing season. The same CCD camera and filters as for the 1995 observations were used. Instrumental profile photometry for stars from the cluster sub-field including OGLEGC17 was derived using the Daophot/Allstar package (Stetson 1987). Standard stars from Landolt (1992) were measured using aperture photometry while aperture corrections for the cluster field were derived using the Daogrow program (Stetson 1990). Based on residuals observed for standard stars and the uncertainties of the derived aperture corrections, we estimate that the total errors of the zero points of our BVI photometry for OGLEGC17 do not exceed 0.02. Numerous sets of observations taken during the 1997 and 1998 observing seasons with a CCD camera on the 1-m Swope telescope at Las Campanas Observatory were used to refine the ephemeris. The final adopted ephemeris is $T_0(HJD) = 2449082.3530 \pm 0.0008$ and $P = 2.4669384 \pm 0.0000023$ days. The 1995 BVI light curves phased with this ephemeris are shown in Figure 1. These light curves contain 181, 197 and 101 data points for the B , V and I -bands, respectively.

On the night of March 16, 1995 (UT) we used the $1K \times 1K$ pixel TEK#1 CCD camera on the du Pont telescope to monitor a primary eclipse of OGLEGC17. The data were reduced in

⁶IRAF is distributed by National Optical Astronomical Observatories, operated by the Association of Universities for Research in Astronomy, Inc., under contract to the National Science Foundation.

an identical fashion as the time series photometry described above. The time resolution of these observations is better than that for the observations collected with the TEK5 camera. The derived V-band light curve is shown in Fig. 2. Note that the eclipse is total, the phase of constant light lasts about 0.035P.

Magnitudes and colors observed at maximum light⁷ and at both minima are listed in Table 1. The totality of the primary eclipse allows a straightforward determination of the magnitudes and colors of both components of the binary. Assuming that to first order effects due to the ellipsoidality of the components and to the reflection of light are negligible one may adopt the magnitudes and colors observed at phase 0.0 (the eclipse of the secondary component) as corresponding to the larger component of the system. Note that we have also assumed that there is no "third light" from an unresolved tertiary component in the OGLEGC17 system. For that star we obtain $V = 17.46$, $B = 18.12$, $I = 16.63$, $B - V = 0.66$ and $V - I = 0.83$. We adopted the convention that the primary component is the one with larger size and luminosity. In this case the secondary component has a smaller size and luminosity but higher surface brightness than its companion. That star is eclipsed at phase 0.0, the deeper minimum. For the secondary component we obtain $V = 18.72$, $B = 19.27$, $I = 17.915$, $B - V = 0.56$ and $V - I = 0.80$. The position of OGLEGC17 in the cluster color-magnitude diagram (CMD) is shown in Fig. 3, where the position of the composite image is shown along with the positions of the individual stars in this binary. The system consists of a main sequence star (secondary component) together with a star which has left its turnoff point (primary component).

2.2. Infrared Photometry

Photometric measurements in the J , H , and K_s passbands were made at random phases in the period 30 January through 7 February 1999. The IRCAM infrared camera (Persson et al. 1992) was used on the du Pont telescope at a scale of 0.348 arcsec/pixel. Observing, linearization, flat-fielding, and sky-frame creation methodologies were closely similar to those detailed in Persson et al. (1998). That paper also presents the definition of the photometric system, standard stars, and filter transmissions. Linearized, sky-subtracted, and photometrically calibrated frames were combined into final stacked images ("mosaics"), which were then photometered with Daophot. The results are presented in Table 2. The uncertainties returned by Daophot are computed from the sky level on the raw data frames, and implicitly take the noise to be Poisson. Measured uncertainties, computed from the dispersion in the individual stellar magnitudes, are typically quite close to the Daophot values, so the latter were adopted and given in Table 2.

The observations were calibrated with observations of standard stars presented in Persson et al. (1998). The data for the first three nights were taken in photometric conditions, and the

⁷As our data do not cover quadratures we list magnitudes and colors observed at phase 0.82

calibration was determined independently for these nights. Photometric zero points for the last three nights were determined by comparing photometry of the other stars in the field of view to an average of the values for the first three nights. The K_s photometric system differs negligibly from that of the Johnson K system for stars of the relevant spectral type. Convolutions of the respective filter transmissions over Kurucz model atmospheres for such stars show typical $K - K_s$ values in the range -0.002 to +0.002.

2.3. Spectroscopy

Echelle observations of OGLEGC17 were obtained with the du Pont 2.5-m telescope between 08 May UT and 13 May UT of 1996. The echelle has a fixed format optical path feeding a 2D-Frutti detector (Sectman 1984). The observations were taken with a 1.5 arcsec slit, and the spectral resolution was about 15 km/sec. A total of 38 spectra were obtained with exposure times of 1800 sec. The spectra were extracted with a set of Fortran programs written at Carnegie Observatories. The final individual extracted spectra had typical signal levels of between 4 and 6 counts at 4490Å. The extracted spectra were reduced to zero heliocentric velocity and binned into nine final spectra according to the ephemeris in Section 2.1.

Echelle observations of OGLEGC17 were also obtained with the Blanco 4-m telescope between 16 April UT and 19 April UT of 1997. Observations were taken with a 1.5 arcsec slit, and the resulting spectral resolution was 14 km/sec with the Red CCD camera. The data were reduced with the echelle package in IRAF. Exposures were 1800 sec, and the 22 individual spectra were coadded into four final spectra according to the ephemeris in Section 2.1.

Multiple observations of the star HD193901 ($B - V = 0.53$, $[\text{Fe}/\text{H}] = -1.2$ (Tomkin et al. 1992)) were obtained at each telescope and reduced with the appropriate software. The individual spectra were averaged to produce a high signal-to-noise template for the velocity measurements. The template spectrum was rotationally broadened to $V_{rot} = 20$ km/sec. Adopting the radii from Section 3, and assuming that the components are rotationally locked, leads to an expected rotational velocities of 38 km/sec for the primary and 18 km/sec for the secondary.

Velocities were measured with the IRAF routine FXCOR. The results are presented in Table 3 where we give the number of spectra averaged at each phase point, the mean phase, the total range in phase, and the velocities and the errors returned from FXCOR. As demonstrated by Latham et al. (1988), all halo binaries with periods less than about ten days have circular orbits. From this, and because of the relative quality of our radial velocity measurements, we assume that OGLEGC17 has a circular orbit (see also the discussion by Lucy and Sweeny (1971)). We made a least squares fit to the velocity data using GaussFit, solving for the systemic velocity γ and the velocity amplitudes K_1 and K_2 . The results of this fit are presented in Table 4. The measured velocities together with the fit are presented in Figure 4. The measured value of γ (237.97 ± 1.93 km/sec) confirms that OGLEGC17 is a member of the cluster, the systemic velocity of ω Cen is

232.3 km/sec (Harris 1996). Adopting an inclination of $i = 86.3$ from the photometric solution in Section 3, we derive $M_1 = 0.806 \pm 0.056 M_\odot$ and $M_2 = 0.686 \pm 0.047 M_\odot$.

3. Photometric solution

The light curves were analysed by use of the Wilson-Devinney (1971; hereafter WD) model as implemented in the 1986 version of the code. The code is described in some detail by Wilson (1979) and by Leung & Wilson (1977). The MINGA minimization package (Plewa 1988).⁸ was used for the actual fitting of the observed light curves and the derivation of system parameters. The bolometric albedo and gravity brightening coefficients were set to values appropriate for stars with convective envelopes: $A_1 = A_2 = 0.5$, $g_1 = g_2 = 0.32$. The mass ratio was fixed to the spectroscopic value $q = m_2/m_1 = 0.851$. We note at this point that because of the well detached configuration of the binary the modeled light curves show only a very small dependence on the assumed value of q . Hence, the uncertainty in q , amounting to 0.073, has little effect on the photometric solutions presented below. In addition, uncertainties in the adopted values of the effective temperatures of the components do not noticeably influence the results of our analysis. These temperatures were estimated using the empirical calibration $T_{eff} = T_{eff}(g, (B-V)_0, [\text{Fe}/\text{H}])$ published by Sekiguchi & Fukugita (2000). The observed colors were corrected for interstellar reddening assuming $E(B - V) = 0.13$ as derived for the coordinates of OGLEGC17 from maps of Schlegel et al. (1998). We adopted $[\text{Fe}/\text{H}] = -1.7$ for the metallicity of OGLEGC17 (see Sec. 4 for discussion of the reddening and the metallicity of OGLEGC17). Theoretical linear limb-darkening coefficients in the BVI bands were taken from Claret, Diaz-Cordoves & Gimenez (1995) and from Diaz-Cordoves, Claret & Gimenez (1995) for the adopted values of effective temperature and metallicity.

We assumed a detached configuration for OGLEGC17 and analysed the light curve by running the WD code in both modes 0 and 2. as described in detail by Leung & Wilson (1977). In Mode 0 the luminosities and temperatures of the components are not coupled. The adjustable parameters are the inclination i , the dimension-less potentials Ω_1 and Ω_2 , and the relative luminosities L_1 and L_2 . The three light curves were analysed simultaneously so the total number of adjustable parameters was equal to nine. In Mode 2 the luminosities are coupled to the temperatures. For that mode the adjustable parameters are i , Ω_1 and Ω_2 , the temperature of the secondary component T_2 , and the luminosity L_1 (a total of 7 free parameters). For both modes stable solutions were derived and the resulting parameters and formal errors are listed in Table 5.

The parameters obtained from both solutions are consistent with each other to within the formal uncertainties. The solution corresponding to Mode 2 shows slightly smaller errors for most parameters and given that this solution has fewer free parameters we adopt it in the following

⁸The MINGA package can be obtained from <http://www.camk.edu.pl/~plewa>

discussion. In Fig. 5 we show the residuals of the fit along with the synthetic light curve overlaid on the observed light curves. In Table 6 we list some of the absolute parameters of the system obtained by combining data from Tables 4 and 5.

The results of our analysis show that OGLEGC17 is a well-detached system. Its primary exhibits a slight ellipsoidality with $r_{pole}/r_{point} = 0.976$.⁹ The secondary component is almost spherical with $r_{pole}/r_{point} = 0.997$. As noted above, the primary is slightly evolved, with a larger total luminosity and lower surface brightness than the secondary.

4. Age determination

The fact that the primary component of OGLEGC17 has already left the cluster turnoff should allow a precise determination of its age by use of age-luminosity and age-turnoff mass relations derived from models of stellar structure and evolution. We adopt the models of Girardi et al. (2000) in the following discussion.

The two main sources of uncertainty in our determination of the age of OGLEGC17 are the relatively large errors in the estimated masses of both components and the metallicity of this particular system. It has been known for many years that unlike other globular clusters in our Galaxy ω Cen contains stars with a range of metallicities (Norris & Bessell 1975). Suntzeff & Kraft (1996) used a sample of 379 stars (234 and 145 from the lower and upper giant branch, respectively) with spectroscopically derived $[\text{Fe}/\text{H}]$ to study the metallicity distribution in the cluster. They found that all but a few stars have $[\text{Fe}/\text{H}]$ ranging from -1.9 to -0.6 ¹⁰. The observed distribution rises rapidly at $[\text{Fe}/\text{H}] = -1.85$ with a median value $[\text{Fe}/\text{H}] = -1.7$. In addition, 78% of their sample has $-1.85 < [\text{Fe}/\text{H}] < -1.4$. A recent study by Majewski et al. (2000) shows quite convincingly that the metallicity distribution of ω Cen giants terminates at the metal-rich end at $[\text{Fe}/\text{H}] \approx -1.15$. The apparent discrepancy with earlier studies is explained by more a careful elimination of field interlopers in the Majewski et al. study.

Unfortunately, our spectra have very low S/N ratio and cannot be used for a direct determination of the system metallicity. However, we can use the location of the components of OGLEGC17 on the cluster CMD (see Fig. 3) to estimate metallicity. Several authors have suggested that ω Cen harbors a few sub-populations of stars, not only of different metallicities but also of different ages (Lee et al. 1999; Hughes & Wallerstein 2000; see also references therein). It has been estimated that ages of the cluster stars cover a range of about 3 Gyr with the more metal rich stars being younger. If this is true then the position of the primary component in the cluster CMD is not very useful as effects of age and metallicity cannot be easily deconvolved at the top of the main-sequence - for a fixed age stars with higher metallicity are fainter, but for fixed $[\text{Fe}/\text{H}]$ younger stars are

⁹ r_{pole} is the "polar" radius while r_{point} is measured in the direction toward the mass center of the binary.

¹⁰We are using the Zinn-West scale of $[\text{Fe}/\text{H}]$ throughout.

brighter. Since the primary component is on the bright side of the "clump" of stars leaving the main-sequence it can be either old and metal poor, or young and metal rich. The secondary component of the binary is located on the blue edge of the upper main-sequence, just below the turn-off. Hence its metallicity places it among the bulk of ω Cen stars with $[\text{Fe}/\text{H}] \approx -1.7$.

In the following discussion we will derive results for two assumed values of metallicity: $[\text{Fe}/\text{H}] = -1.74$ and $[\text{Fe}/\text{H}] = -1.33$. The lower value is marginally smaller than the median value for the bulk of the cluster giants (Suntzeff & Kraft 1996) and the higher one marks the lower end of the observed metallicity distribution. In addition, modern evolutionary tracks suitable for our analysis are available in the literature for these two values of $[\text{Fe}/\text{H}]$ (see below).

4.1. Age - Turnoff Mass Relations

The most straightforward way to estimate the age of the cluster is to use the fact that the mass of the primary star in OGLEGC17 differs negligibly from the turnoff mass of ω Cen. The time it takes a main sequence star to exhaust its core hydrogen is a monotonic function of mass therefore our estimate of the mass of the primary star derived from spectroscopic and photometric data can be used to directly measure the age of the cluster.

Figure 6 shows age - turnoff mass relations from Girardi et al. (2000) for metallicities $Z = 0.0004$ and $Z = 0.001$, corresponding to $[\text{Fe}/\text{H}] = -1.74$ and $[\text{Fe}/\text{H}] = -1.33$, respectively, assuming $\log Z = 0.977[\text{Fe}/\text{H}] - 1.699$ (Bertelli et al. 1994). These values bracket the likely value for the metallicity of OGLEGC17. The solid line and dotted lines represent the mass of the primary star and one sigma errors, $0.806 \pm 0.056 M_{\odot}$. The resulting ranges in the age of the primary of OGLEGC17 are $9.1 < t_1 < 15.8$ Gyr for $Z = 0.0004$, and $9.5 < t_1 < 16.7$ Gyr for $Z = 0.001$. A formal error in the estimated age of ± 1 Gyr could be obtained by reducing the uncertainties in the masses to $\pm 0.015 M_{\odot}$. The corresponding uncertainty in the $K_{1,2}$ velocities is ± 1 km/s.

4.2. Age - Luminosity Relations

We can also estimate the age of the cluster by using age versus luminosity relations. An advantage of this approach is that the parameters of the secondary component provide an independent constraint on the age of the binary and therefore can be used for testing and/or improving the result derived from analysis of the primary component alone. To minimize the uncertainties involved in a comparison of observed quantities with calibrations provided by models we use the age versus bolometric luminosity relation (Girardi et al. 2000). Bolometric luminosities from models are unaffected by uncertainties associated with model isochrones relating T_{eff} and L_{bol} to color index and absolute magnitude in a selected band. First we have to determine bolometric luminosities for both components. We calculate these from the standard relation $L_{bol} = 4\pi R^2 \sigma T_{eff}^4$. Two recent empirical calibrations of $T_{eff} = T_{eff}(g, [Fe/H], B - V)$ have been published by Alonso et al. (1996)

and by Sekiguchi & Fukugita (2000; SF hereafter). These are in good agreement with each other. For the range of colors and metallicities discussed below, the calibration by Alonso et al. (1996) gives values of T_{eff} which are systematically lower by 25-30 deg than the T_{eff} based on the SF calibration. That difference has only a small impact on calculated L_{bol} (as compared with errors associated with uncertainties of radii, $E(B - V)$ and $B - V$) and therefore we will use values of T_{eff} based on the SF calibration. To estimate T_{eff} we need to know both $(B - V)_0$ and $[Fe/H]$.

The Harris catalogue (Harris 1996) gives $E(B - V) = 0.12$ for ω Cen. According to maps of the extinction by Schlegel et al (1998) $E(B - V)$ varies by about 0.02 across the field of the cluster, with the reddening slightly larger in the southern part of the cluster. For the position of OGLEGC17 we get $E(B - V) = 0.132$. We will adopt for our analysis $E(B - V) = 0.13 \pm 0.02$. Assuming 0.02 as an error of our $B - V$ measurements we have $(B - V)_{0,1} = 0.53 \pm 0.03$ and $(B - V)_{0,2} = 0.43 \pm 0.03$.

We also calculate the bolometric luminosities of the components of OGLEGC17 using calibrations of $T_{eff} = T_{eff}([Fe/H], V - K)$ from Alonso et al. (1996, 1999) for dwarf and giant stars. As discussed in Section 5.2, we have to assume values for the luminosity ratios for the two components in OGLEGC17 because we do not have infrared observations of the eclipse profiles. Adopting the luminosity ratios given in Section 5.2, and assuming a reddening of $E(B - V) = 0.13 \pm 0.02$, we derive $(V - K)_0 = 1.40$ for the primary and $(V - K)_0 = 1.17$ for the secondary.

In Table 7 we list the effective temperatures derived for both components of OGLEGC17 using the SF and Alonso et al. calibrations for metallicities $Z = 0.0004$ and $Z = 0.001$. For each component we list the formal errors in T_{eff} including a 0.03 uncertainty $(B - V)_0$ as well as an rms error from the color - effective temperature calibration. These values of T_{eff} and the absolute radii listed in Table 6 are used to calculate the bolometric luminosities. The resulting values of L_{bol} along with their formal errors are given in the last two columns of Table 7.

The luminosity of a star of a given mass is a function of 3 parameters: age t , initial metallicity Z and initial helium abundance Y . While Z (or more precisely $[Fe/H]$) can be relatively easily determined from the observations, the helium abundance cannot be measured directly in main sequence stars of globular clusters. In the case of a binary star whose components have the same initial composition there is, however, some redundancy of information. Hence, knowing the masses of both components and $[Fe/H]$ we may determine both Y and t from the observed luminosities ¹¹. A more thorough discussion of this subject is given by Paczynski (1997).

In Figure 7 we show age versus luminosity relations based on evolutionary tracks recently published by Girardi et al. (2000). The left panel is for models with $[Z = 0.0004, Y = 0.23]$ while the right one is for $[Z = 0.001, Y = 0.23]$. In each panel we show relations for the primary star mass \pm one sigma errors ($m_1 = 0.806 \pm 0.056 M_\odot$ with dotted lines and relations for the secondary

¹¹To be precise, such a procedure is applicable only to detached systems which have not undergone any mass transfer episodes during their evolution

mass \pm one sigma errors ($m_2 = 0.686 \pm 0.047 M_\odot$) with solid lines. These relations were derived from evolutionary tracks for $m/m_\odot = 0.6, 0.7, 0.8, 0.9$, interpolating to the appropriate mass using a method developed by Weiss and Schlattl (2000). Vertical lines in Figure 7 mark $L \pm \sigma_L$ ranges for L_1 and L_2 . The intersections of age - luminosity relations with lines marking 1 sigma limits on L_1 and L_2 give limits on the age for a given mass. For the $B - V$ effective temperature calibration and $Z = 0.0004$ we obtain $9.1 < t_1 < 17.0$ Gyr for the primary component of OGLEGC17. For the secondary component we adopt a conservative lower limit to the age corresponding to the age at the lower one sigma values of mass and luminosity: $t_2 > 12.9$ Gyr. This leads to a plausible age of the binary $12.9 < t < 17.0$ Gyr. Similarly for $Z = 0.001$ we obtain $9.8 < t_1 < 18.4$ Gyr and $t_2 > 14.9$ Gyr leading to an age of $14.9 < t < 18.4$ Gyr. For the $V - K$ effective temperature calibration and $Z = 0.0004$ we obtain $9.6 < t_1 < 17.1$ Gyr for the primary component. For the secondary component we find $t_2 > 15.0$ Gyr. This leads to a plausible age of the binary $15.0 < t < 17.1$ Gyr. Similarly for $Z = 0.001$ we obtain $10.4 < t_1 < 18.5$ Gyr and $t_2 > 16.4$ Gyr leading to an age of $16.4 < t < 18.5$ Gyr.

Our limits on the age of the primary do not depend strongly on metallicity or which color is used to determine the effective temperatures. In all cases, the derived age of the secondary reduces the limits on the ages. We conclude that for the masses and luminosities derived for both components of OGLEGC17 the age of the binary can be constrained to the approximate range $12.9 < t < 18.5$ Gyr.

We note that accurate determination of t_2 would require narrowing of errors for both m_2 and L_2 . However, an improved estimate of t_1 is possible just by narrowing a range of allowable values of m_1 . This is due to fact that the primary component has already reached an evolutionary stage at which luminosity is a steep function of age. Within the formalism of our age estimate, a reduction in the error in the age to ± 1.0 Gyr would require improving the error in the K velocities to approximately ± 0.5 km/sec, a value that should be easily achievable with observations of OGLEGC17 with the new generation of echelle spectrographs on southern large telescopes (eg. Torres et al. 1997; Metcalfe et al. 1996). These data would lead to accuracies in the masses and absolute radii of better than one per cent. In addition, the systematic error associated with the uncertain metallicity of this system can be addressed by high signal-to-noise echelle observations at quadrature, where the relative velocities of the two components are large enough to allow an metallicity estimate for each of the components.

4.3. Dependence of derived ages on stellar models

The limits on the age of OGLEGC17 listed above were derived using stellar tracks taken from models published by Girardi et al. (2000). One may wonder to what extent our results depend on the selection of a particular set of stellar models. A detailed comparison of different sets of models is beyond the scope of this paper. However, we performed a limited test by comparing age-luminosity relations from Girardi et al. (2000) with relations constructed from tabular data

given by Weiss & Schlattl (2000). Analytical expressions given by Weiss & Schlattl allow one to construct age-luminosity relations for a large range of masses and chemical composition defined by Z, Y . Hence, given masses and luminosities for the components of a given binary, one may derive not only the age but also the helium content Y . Age-luminosity relations were extracted from two sets of models for $[Z, Y] = [0.0004, 0.23]$ and for $[Z, Y] = [0.001, 0.23]$ and for masses $0.7M_{\odot}$ to $0.8M_{\odot}$. A comparison of these two sets of models is presented in Figure 8 which shows differential residuals δt versus luminosity for models with $[Z, Y] = [0.0004, 0.23]$ and for two values of the mass. We conclude that relations based on these two recent sets of models are in very good agreement with each other for the considered range of parameters.

5. Distance to the cluster

OGLEGC17 offers the opportunity for determining the distance to a globular cluster in a way independent of other measurement techniques. Here we present two estimates, one based on the bolometric luminosities of the components of the binary, and the second based on relations between the surface brightness and infrared colors.

5.1. Bolometric Luminosities

We may use the bolometric luminosities listed in Table 7 to calculate the absolute visual magnitudes M_V of both components of the binary. Bolometric corrections were obtained by interpolating tabular data given in (Houk et al. 2000) for unreddened color indices $(B - V)_{0,1} = 0.53$ and $(B - V)_{0,2} = 0.43$ and gravities $\log g_1 = 3.8$ and $\log g_2 = 4.4$. We obtained bolometric corrections $BC_1 = -0.22$ and $BC_2 = -0.21$ for $[\text{Fe}/\text{H}] = -1.74$ and $BC_1 = -0.20$ and $BC_2 = -0.19$ for $[\text{Fe}/\text{H}] = -1.33$. Our formal uncertainties of $(B - V)_0$ of 0.03 transform into formal errors for bolometric corrections of about 0.01. Adopting $M_{bol\odot} = 4.70$ (eg. Salaris & Weiss 1988) and using the bolometric luminosities from Table 7 we arrive at the absolute visual magnitudes given in Table 8. We then use the apparent V magnitudes of both components to calculate the distance moduli and these are also given in Table 8. Values of $(m - M)_V$ derived for the primary and the secondary component are consistent with each other. For the $(B - V)$ effective temperature calibration and $[\text{Fe}/\text{H}] = -1.74$ we obtain an average value $(m - M)_V = 13.78 \pm 0.16$ while for $[\text{Fe}/\text{H}] = -1.33$ we have $(m - M)_V = 13.86 \pm 0.16$. For the $(V - K)$ effective temperature calibration and $[\text{Fe}/\text{H}] = -1.74$ we obtain an average value of $(m - M)_V = 14.00 \pm 0.09$ and for $[\text{Fe}/\text{H}] = -1.33$ we obtain $(m - M)_V = 14.00 \pm 0.09$.

These values are broadly consistent with $(m - M)_V = 13.84$ adopted by Harris (1996) for ω Cen.

5.2. Surface Brightnesses

We estimate the distance to OGLEGC17 by use of empirically calibrated relations between surface brightness and infrared color. Di Benedetto (1998) presented a calibration of S_V vs $(V - K)$ for a sample of nearby, Population I stars with luminosity classes III, IV, and V. We have extended his calibration to $V - I$, $V - J$, and $V - H$ for the same set of stars.

Figure 9 presents these photometric data, together with quadratic least-squares fits. Values for S_V and for $(V - K)_0$ were taken from Di Benedetto (1998), and the rest of the photometric data were taken from archival tables accessed at the Centre de Données astronomiques de Strasbourg. Note that the calibrating photometry is in the Johnson system. The terms for the quadratic fits are presented in Table 9 together with the rms values of the fits (some obviously discrepant points in Figure 9 were not included in these fits). Figure 9 also shows reddening vectors for a reddening of $A_V = 1.0$. The vectors are essentially parallel to the relations, indicating that modest errors in the reddening do not impact the estimates of the physical distance to the binary (note, however, that errors in the reddening do directly affect the final estimates of the distance modulus $(m - M)_V$). Given the relative rms values of the fits, and the steepness of the $S_V - (V - I)$ relation, we estimate the distance to OGLEGC17 using only our J , H , and K -band data.

The stars used in the surface brightness calibration are of necessity in the solar neighbourhood, and therefore most likely are Population I stars. To see how the surface brightness versus color calibration depends on metallicity we have used synthetic color-temperature relations from Houdashelt et al. (2000). Figure 10 presents S_V - color relations extracted from Table 5 in Houdashelt et al. (2000) for $[\text{Fe}/\text{H}] = 0.0$ and $[\text{Fe}/\text{H}] = -2.0$. As also found by Di Benedetto (1998), these relations show little sensitivity to metallicity, the correction amounting to approximately +0.04 in S_V for the J filter and +0.02 in S_V for the H and K filters.

Table 2 presents mean magnitudes for J , H , and K -band observations of OGLEGC17 taken out of eclipse. Assuming $V = 17.155$ for OGLEGC17 at quadrature, and assuming a reddening of $E(B - V) = 0.13$ and a reddening law from Rieke and Lebofsky (1985) we calculate the mean colors for the system as a whole listed in column 2 of Table 10. The WD solution for the light curve (see Figure 5) indicates that the ellipticity of the primary and, to a lesser extent, reflection effects in the binary, produce a one percent modulation of the V -band light out of eclipse. We have ignored these effects in calculating mean colors. In order to calculate the colors of the individual components we need to know the relative luminosities of the primary and secondary. These ratios require light curves through the eclipses in the infrared bands, data which we do not have. The WD code used to estimate these ratios by extrapolating the B , V , and I -band solutions to J , H , and K (Mode 2, see Table 5). These values are $q_J = 3.922$, $q_H = 4.038$, and $q_K = 4.136$ with estimated errors of ± 0.05 . The unreddened colors of the individual components of the binary are listed in columns 3 and 4 of Table 10.

The surface brightness S of a star is defined as:

$$m_0 = S - 5 \log \phi \tag{1}$$

where m_0 is the un-reddened apparent magnitude of a star of angular diameter ϕ . The zero-point is set such that $S = m_0$ for $\phi = 1$ mas. From Di Benedetto, equation 4, we have

$$\phi(mas) = 10^{(S_V - 0.2*(V - A_V))}, \tag{2}$$

and from Lacy (1977), equation 4, we have

$$d(pc) = 1.337 \times 10^{-5} r(km) / \phi(mas). \tag{3}$$

Also

$$(m - M)_V = 5.0 * \log(d(pc)) - 5.0 + A_V. \tag{4}$$

We use colors from Table 10 (transformed to the Johnson system using relations in Persson et al. (1998) and Bessel and Brett (1988)) together with the relations in Table 9 to calculate the surface brightnesses of the components of the binary; these are listed in columns 2 and 3 in Table 11. The above equations are then used to calculate the distances (columns 4 and 5 in Table 11) and the distance moduli (columns 6 and 7 in Table 11).

We adopt a distance which is the average of the values derived for the S_V estimates from $V - J$, $V - H$, and $V - K$ for the primary and secondary, all values weighted equally. The final values are $d = 5469$ pc and $(m - M)_V = 14.09$. To estimate the errors in these values we determined the sensitivity of the answers to one sigma variations in the input observations. The physical distance changes 4.0 per cent for a one sigma change in K_1 and K_2 , 2.9 per cent for $r_1/(a_1 + a_2)$ and $r_2/(a_1 + a_2)$, 2.2 per cent for J , H , and K photometry, 0.8 per cent for V photometry, and 0.7 per cent for $E(B - V)$. The result is insensitive (0.3 per cent change) to variations in q_V , q_J , q_H , and q_K . The quadrature sum of these percentage errors totals 5.5 per cent, and our final estimate of the distance to ω Centauri is 5385 ± 300 pc. The distance modulus is $(m - M)_V = 14.06 \pm 0.11$. Note that the error in the reddening is much more important in determining the distance modulus. It is interesting to note that the values for the distance modulus derived from our K -band observations (through bolometric luminosities using effective temperatures calibrated with $V - K$ colors and through surface brightnesses estimated from $V - J$, $V - H$, and $V - K$ colors) are very similar and differ at the level of 0.20 magnitudes from the other estimates of the distance modulus of ω Cen.

5.3. Discussion

The error in the estimation of the physical distance is dominated by the accuracy of the velocity curve and the accuracy of the photometric solution for the radii. As mentioned in the previous

section, it should be possible to lower the errors in the radial velocity curve by at least a factor of five by use of improved echelle observations of OGLEGC17. In addition, detailed visual and infrared observations of the light curves will improve the photometric solution for relative radii and luminosities. Given that the primary eclipse is total and that the binary is detached, a precision of the order of 0.1% is attainable for these relative parameters. In addition, we will be able to replace the estimates of the effective temperatures based on $(B - V)$ with superior estimates based on infrared colors, significantly reducing errors arising from uncertain metallicity of OGLEGC17.

6. Summary

We have presented photometric and spectroscopic observations of the detached, eclipsing binary OGLEGC17 in the globular cluster ω Cen. We have used these data to estimate the age of this system to be $9.1 < t < 16.7$ Gyr from age - turnoff mass relations and $12.9 < t < 18.5$ Gyr from age - luminosity relations. We have used an empirical calibration of surface brightness with infrared color to estimate a distance of 5385 ± 300 pc to the cluster, a distance modulus of $(m - M)_V = 14.06 \pm 0.11$. This is in disagreement with an estimate of $(m - M)_V = 13.79$ based on the measured bolometric luminosities of the components of the binary.

These estimates can be improved in a straightforward way by further observations, in particular better determinations of the K_1, K_2 velocities and of the visual and infrared eclipse light profiles. Formal errors in the age of ± 1 Gyr are achievable by reducing the errors in the velocity curves to ± 1 km/s.

JK and WP were supported by the Polish Committee of Scientific Research through grant 2P03D003.17 and by NSF grant AST-9819787 to Bohdan Paczyński. IT, SEP and GWP were supported by NSF grant AST-9819786. JK thanks Robert Lupton for his continuing interest in the progress of this work.

REFERENCES

- Alonso, A., Arribas, S., & Martinez-Roger 1996, A&A, 313, 873
Alonso, A., Arribas, S., & Martinez-Roger 1999, A&AS, 140, 261
Anderson, J. 1991, A&A Rev., 3, 91
Barnes, T. G., and Evans, D. S. 1976, MNRAS, 174, 489
Bell, S. A., Hill, G., Hilditch, R. W., Clausen, J. V., and Reynolds, A. P. 1993, MNRAS, 265, 1047
Bertelli, G., Bressan, A., Chiosi, C., Fagotto, F., & Nasi, E. 1994, A&AS, 106, 275

- Bessel, M. S. & Brett, J. M. 1988, PASP, 100, 1134
- Claret, A., Diaz-Cordoves, J., & Gimenez, A. 1995, A&AS, 114, 247
- Diaz-Cordoves, J., Claret, A., & Gimenez, A. 1995, A&A, 110, 329
- Di Benedetto, G. P. 1998, A&A, 339, 858
- Fitzpatrick, E. L., Ribas, I., Guinan, E. F., DeWarf, L. E., Maloney, F. P., & Massa, D. 2001, ApJ, in press
- Girardi, L., Bressan, A., Bertelli, G., & Chiosi, C. 2000, A&AS, 141, 371
- Guinan, E. F. et al. 1998, ApJ, 509, L21
- Hajian, A. R. et al. 1998, ApJ, 496, 484
- Houdashelt, M.J., Bell, R.A., & Sweigert, A. V. 2000, AJ, 119, 1448
- Harris, W. E. 1996, AJ, 112, 1487
- Hughes, J., & Wallerstein, G. 2000, AJ, 119, 1225
- Kaluzny, J. K., Kubiak, M., Szymański, M., Udalski, A., Krzemiński, and Mateo, M. 1996, A&AS, 120, 139
- Kaluzny, J. K., Wysocka, A., Stanek, K., and Krzemiński, W. 1998, Acta Astronomica, 48, 439
- Kruszewski, A. & Semeniuk, I. 1999, Acta Astronomica, 49, 561
- Lacy, C. H. 1977, ApJ, 213, 458
- Lacy, C. H. 1979, ApJ, 228, 817
- Landolt, A. 1992, AJ, 104, 340
- Latham, D. W., Mazah, T., Carney, B. W., McCroskey, R. E., Stefanik, R. P., and Davis, R. J. 1988, AJ, 96, 567
- Lee, Y.-W., Joo, J.-M, Sohn, Y.-J., Rey, S.-C., Lee, H.-C., & Walker, A.R. 1999, Nature, 402, 55L
- Leung, K.-C., & Wilson, R.E. 1977, ApJ, 211, 853
- Lucy, L. B. and Sweeny, M. A. 1971, AJ, 76, 544
- Majewski, S.R., Petterson, R.J., Dinescu, D.I., Johnson, W.Y., Ostheimer, J.C., Kunkel, W.E., & Palma, C. 2000, in The Galactic Halo: From Globular Clusters to Field Stars, ed. A.Noels et al. (Liege: Univ. Liege, Inst. d’Astrophys.Geophys.), in press ; /astro-ph/9910278
- Metcalf, T.S., Mathieu, R.D., Latham, D.W., & Torres, G. 1996, ApJ, 456, 356

- Norris, J., & Bessell, M.S. 1975, *ApJ*, 211, L91
- Paczyński, B. 1997, *The Extragalactic Distance Scale STScI Symposium*, (Cambridge: Cambridge University Press)
- Perryman, M. A. C. et al. 1997, *A&A*, 323, L49
- Persson, S. E., West, S. C., Carr, D. M., Sivaramakrishnan, A., and Murphy, D. C. 1992, *PASP*, 104, 204
- Persson, S. E., Murphy, D. C., Krzeminski, W., Roth, M., and Rieke, M. J. 1998, *AJ*, 116, 2475
- Plewa, T. 1988, *Acta Astron.*, 38, 415
- Reid, I. N. 1998, *AJ*, 115, 204
- Renzini, A. 1991 in *Observational Tests of Cosmological Inflation*, edited by T. Shanks et al. (Dordrecht: Kluwer), 131
- Rieke, G., & Lebofsky, M. 1985, *ApJ*, 288, 618
- Salaris, M., & Weiss, A. 1998, *A&A*, 335, 943
- Schechter, P. S., Mateo, M., and Saha, A. 1993, *PASP*, 105,1342
- Shectman, S. A. 1984, *Instrumentation in Astronomy V*, *Proc SPIE*, edited by A. Boksenberg and D. L. Crawford (SPIE, Bellingham), 445, 128
- Schlegel, D.J., Finkbeiner, D.P., Davis, M. 1998, *ApJ*, 500, 525
- Semeniuk, I. 2000, *Acta Astronomica*, 50, 381
- Sekiguchi, M., & Fukugita, M. 2000, *AJ*, 120, 1072
- Stebbins, J. 1910, *ApJ*, 32, 185
- Stetson, P.B. 1987, *PASP*, 99, 191
- Stetson, P.B. 1990, *PASP*, 102, 932
- Suntzeff, N.B., & Kraft, R.P. 1996, *AJ*, 111, 1913
- Tokunaga, A.T. 2000, in *Allens's Astrophysical Quantities*, ed. A.N. Cox, p. 143 (Springer-Verlag)
- Tomkin, J., Lemke, M., Lambert, D. L., and Sneden, C. 1992, *AJ*, 104, 1568
- Torres, G., Stefanik, R.P., Andersen, J., Nordstrom, B., Latham, D., & Clausen, J.V. 1997, *AJ*, 114, 2764
- VandenBerg, D. A., Bolte, M., and Stetson, P. B. 1996, *ARA&A*, 34, 461

Weiss, A., & Schlattl, H. 2000, A&AS, 144, 487

Wilson, R.E. 1979, ApJ, 234, 1054

Wilson, R.E., & Devinney, E.J. 1971, ApJ, 166, 605

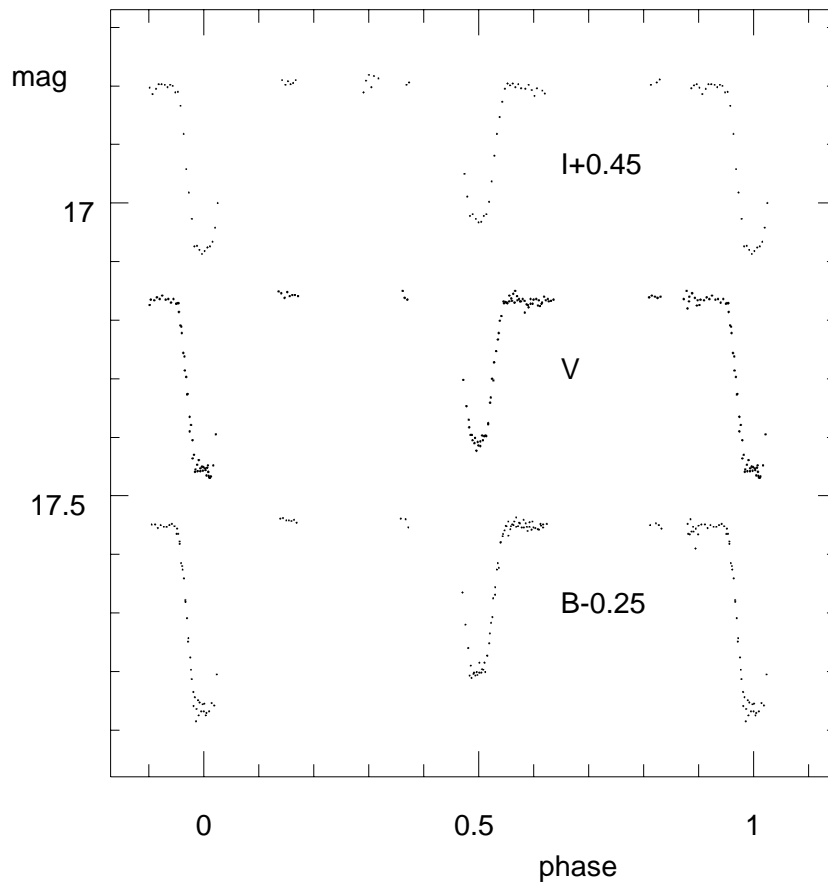


Fig. 1.— *BVI* light curves of OGLEGC17.

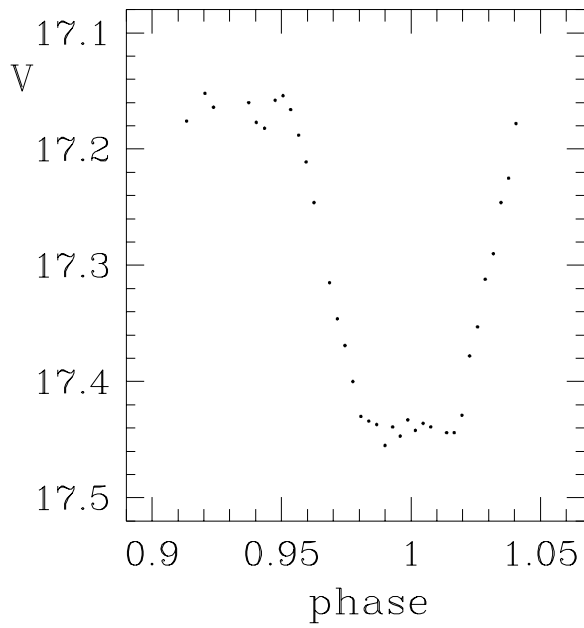


Fig. 2.— The V-band light curve of OGLEGC17 obtained with the TEK1 camera.

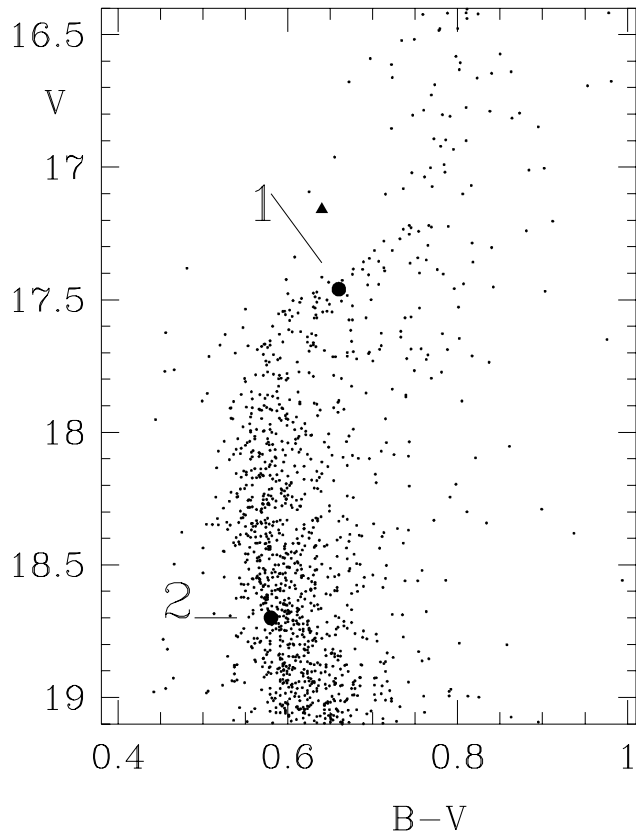


Fig. 3.— The ω Cen CMD for stars near OGLEGC17. The locations of both components of the binary are marked along with the position of the composite image (filled triangle).

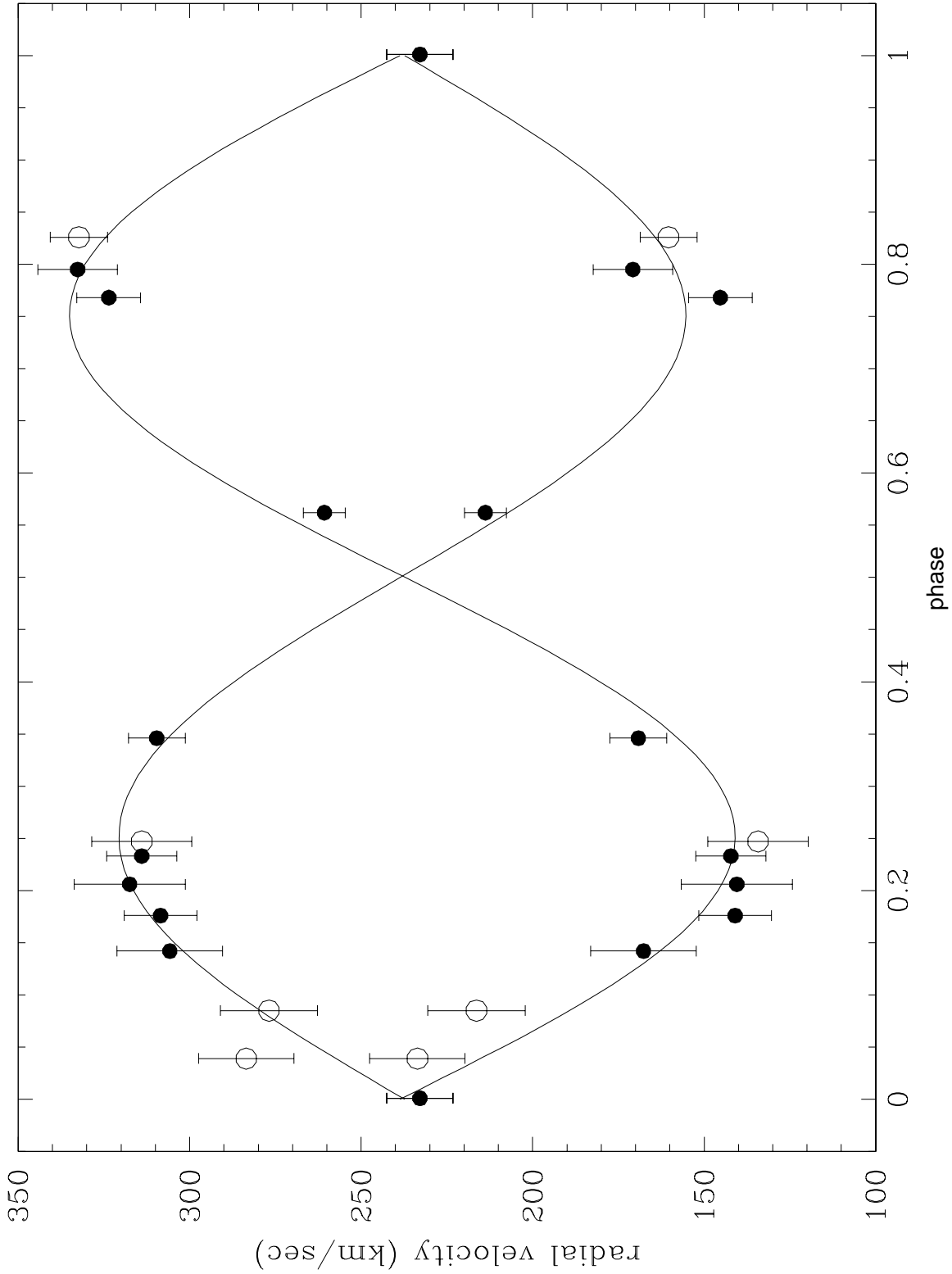


Fig. 4.— The LCO (filled symbols) and CTIO (open symbols) radial velocities plotted with the GaussFit orbital solution.

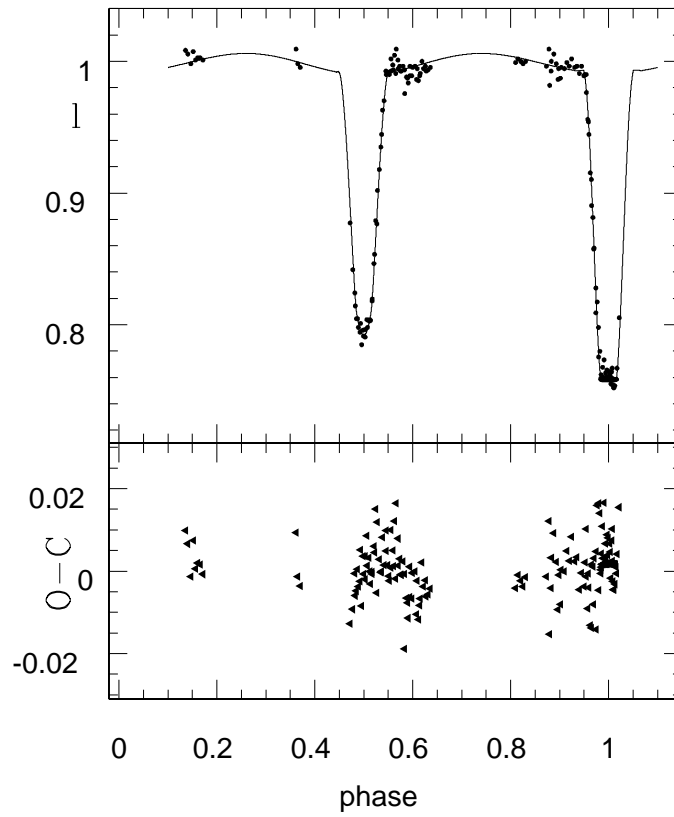


Fig. 5.— The observed V -band light curve (in intensity units) overplotted with the photometric solution. Residuals for the solution in Mode 2 are shown at the bottom.

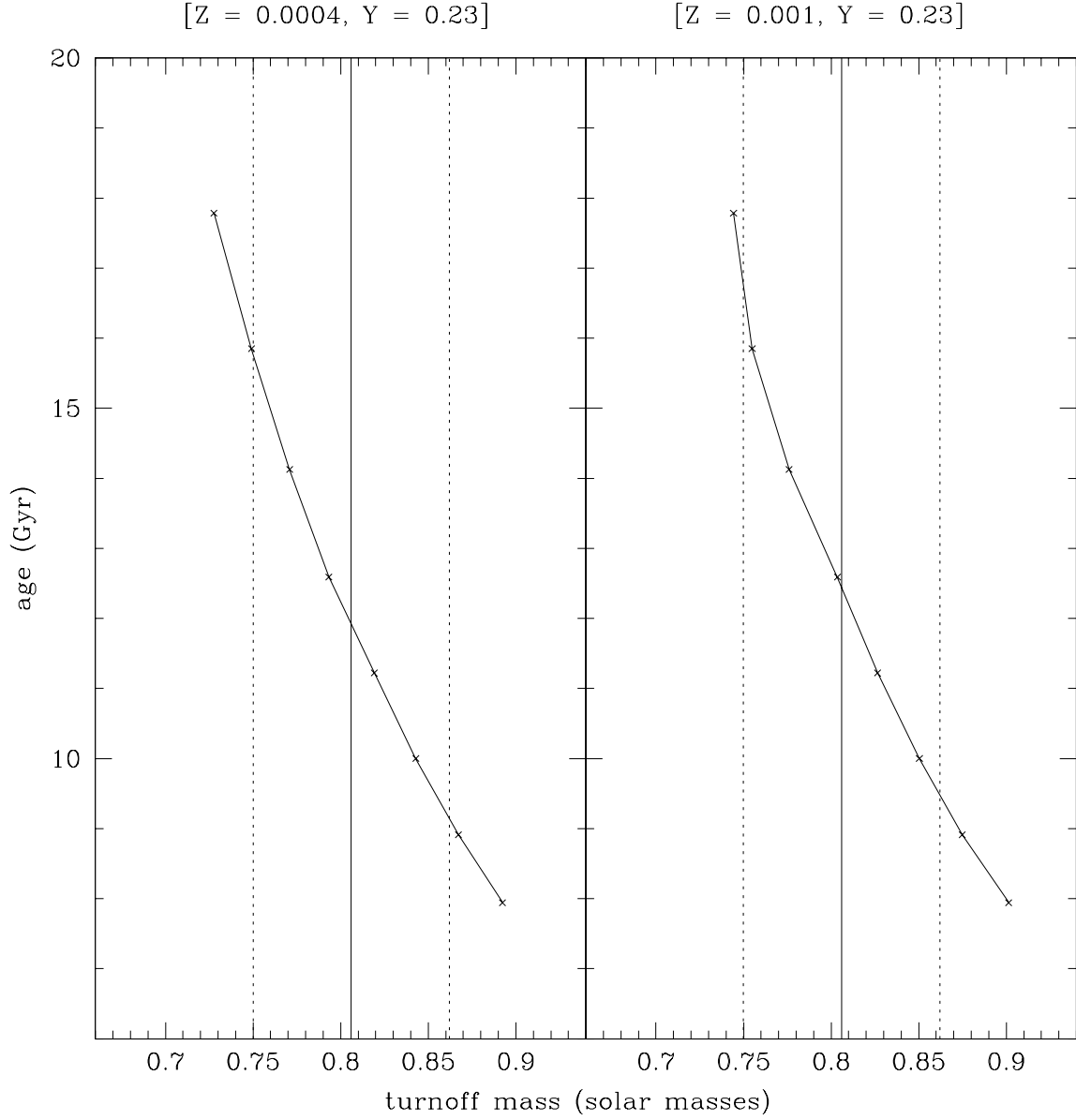


Fig. 6.— Age - turnoff mass relations from Girardi et al. (2000). The left panel is for $Z = 0.0004$, $Y = 0.23$ and the right panel is for $Z = 0.001$, $Y = 0.23$. The vertical solid line represents the mass of the primary of OGLEGC17 and the vertical dotted lines represent one sigma errors in the mass.

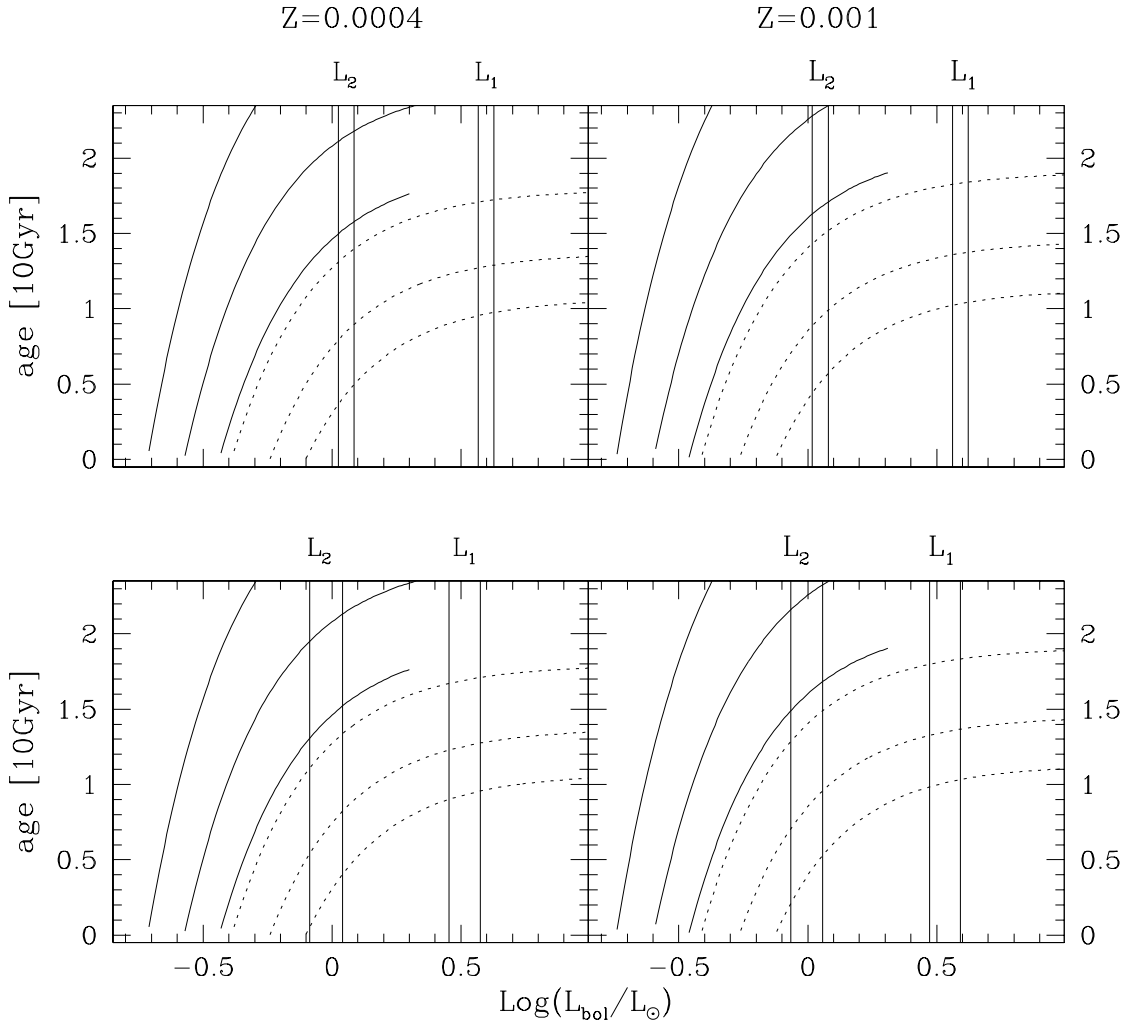


Fig. 7.— Theoretical age-luminosity relations for masses $m_2 = 0.686 \pm 0.046 M_{\odot}$ (continuous curves) and $m_1 = 0.806 \pm 0.056 M_{\odot}$ (dotted curves) from Girardi et al. (2000). Vertical lines mark \pm one sigma ranges for the observed luminosities of the components of OGLEGC17. The upper panel corresponds to bolometric luminosities derived with a $V - K$ calibration of effective temperatures. The lower panel corresponds to bolometric luminosities derived with a $B - V$ calibration. See text for details.

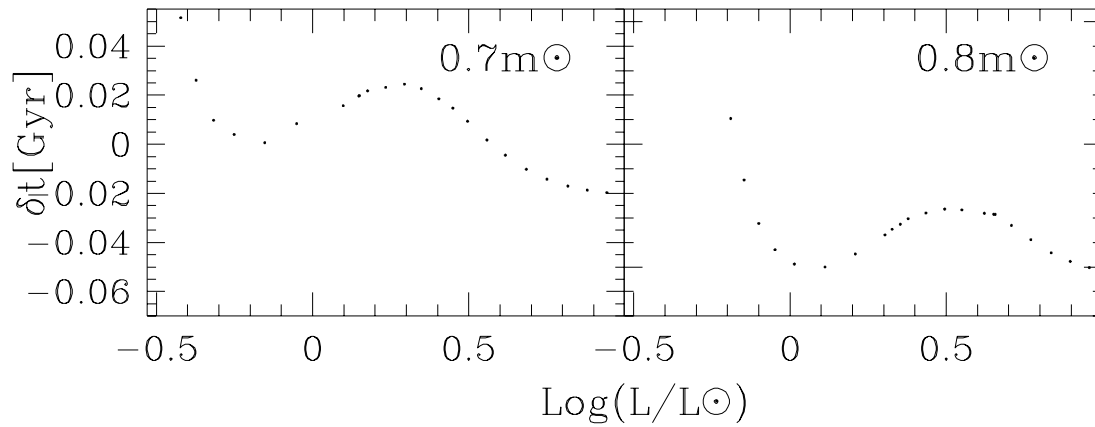


Fig. 8.— Differences between age-luminosity relations from Girardi et al. (2000) and Weis & Schlattl (2000). Difference in age predicted for a given luminosity are shown for masses $0.7m_{\odot}$ and $0.8m_{\odot}$ and for models with $Z=0.001$ and $Y=0.23$.

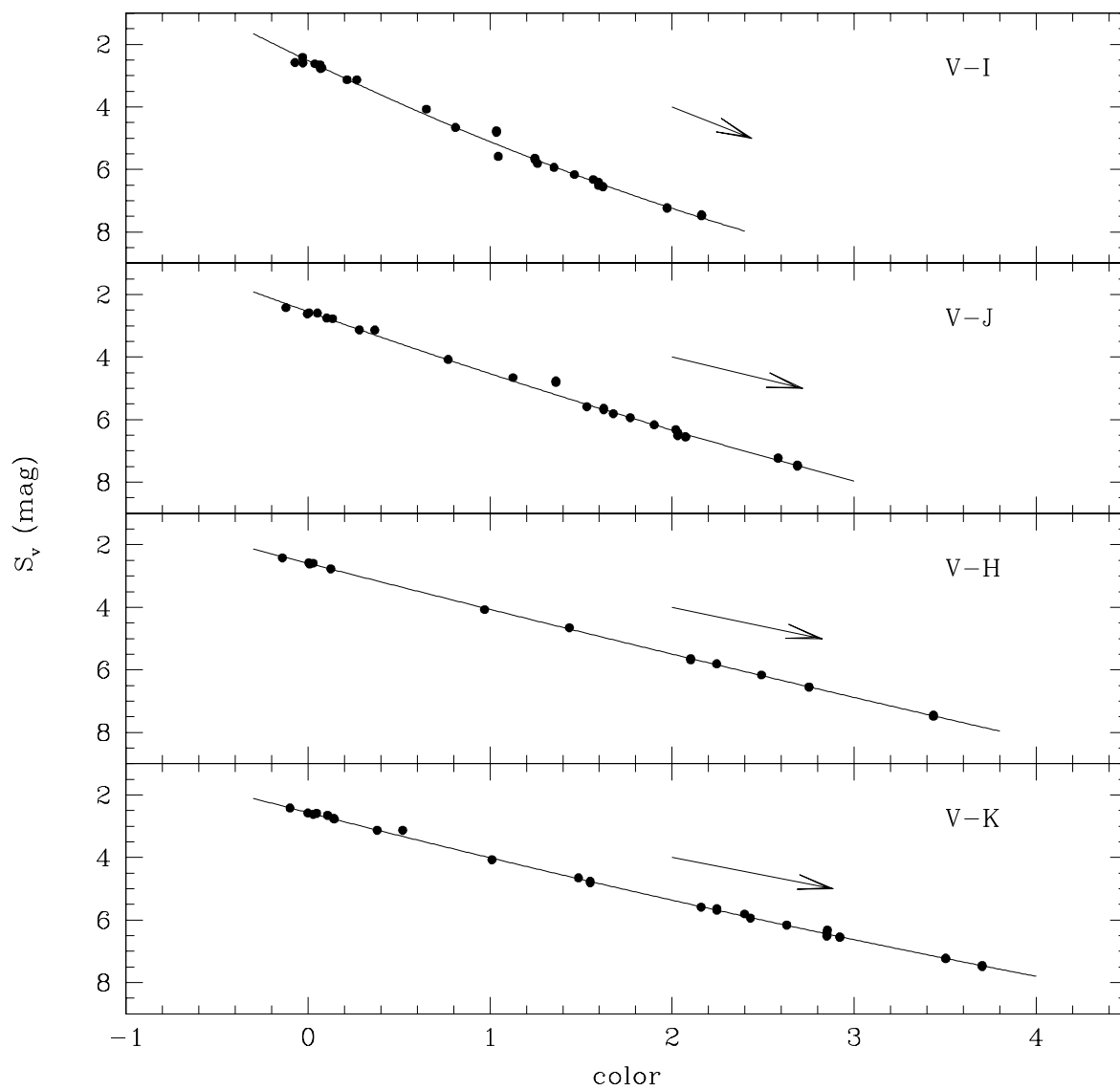


Fig. 9.— The surface brightnesses of nearby stars in the V -band is plotted against $V-I$, $V-J$, $V-H$, and $V-K$ colors. The solid lines are quadratic least-squares fits to the data, the coefficients of the fits are listed in Table 9. The arrows correspond to a reddening A_V of one magnitude.

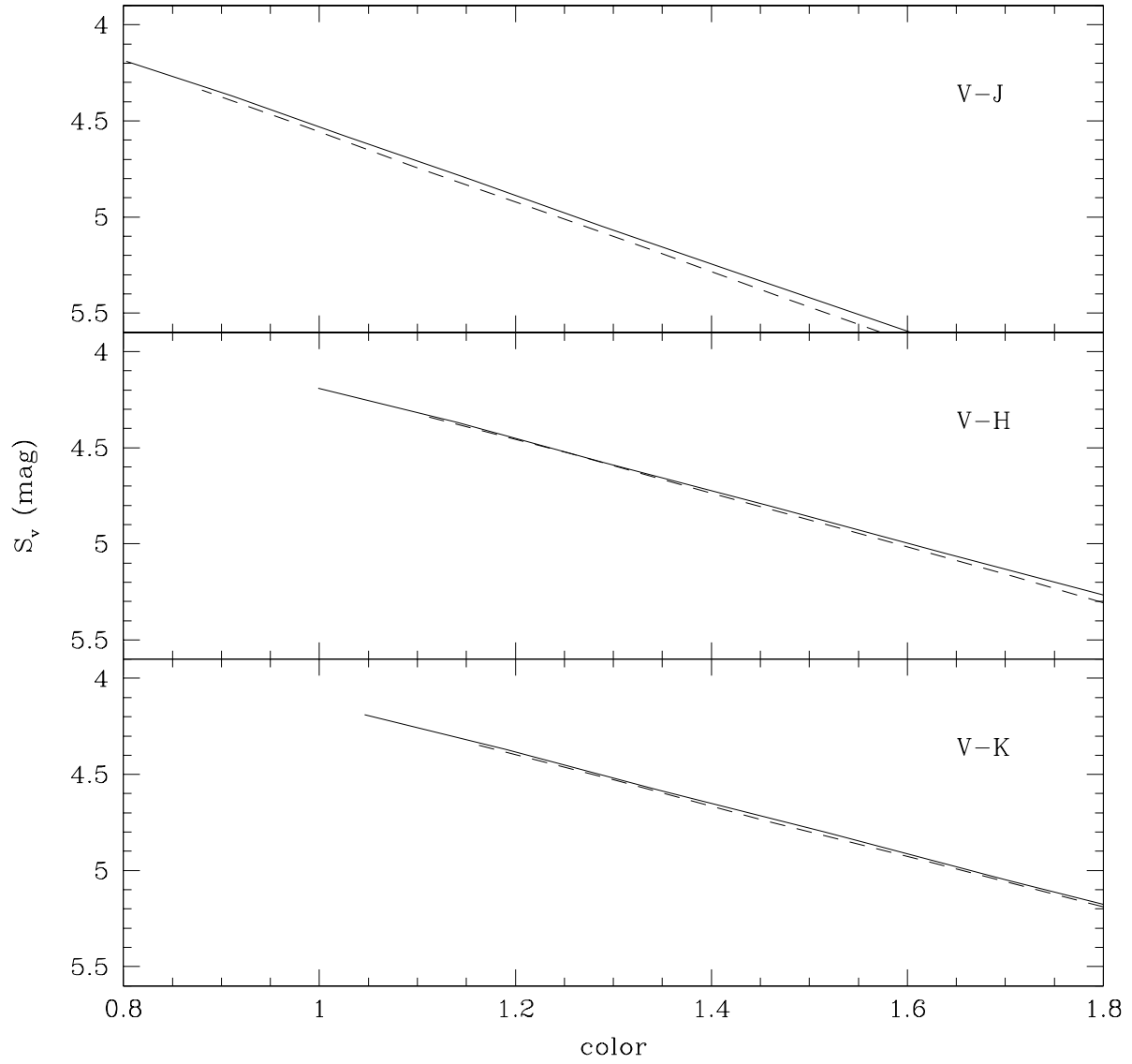


Fig. 10.— Synthetic relations $S_V-(V - K)$ for $[\text{Fe}/\text{H}] = 0$ (solid lines) and $[\text{Fe}/\text{H}] = -2.0$ (dotted lines).

Table 1. BVI photometry of OGLEGC17 at minima and at quadrature

phase	V	B	I	$B - V$	$V - I$
Max	17.155	17.790	16.340	0.635	0.815
Min I	17.450	18.110	16.63	0.66	0.82
Min II	17.41	18.050	16.58	0.640	0.83

Table 2. Infrared photometry of OGLEGC17

HJD ^a	phase	J	phase	H	phase	K_s
09.849	0.403	15.82±0.02	0.396	15.47±0.02	0.392	15.42±0.02
11.882	0.228	15.85±0.02	0.225	15.49±0.01	0.217	15.41±0.03
12.877	0.631	15.90±0.01	0.627	15.50±0.01	0.617	15.48±0.02
14.792	0.407	15.89±0.02	0.410	15.49±0.02	0.419	15.44±0.03
16.872	0.250	15.86±0.02	0.246	15.48±0.03	0.233	15.46±0.02
17.780	0.618	15.88±0.02	0.621	15.50±0.02	0.629	15.48±0.03
average		15.867±0.029		15.488±0.012		15.448±0.030

^aHJD for J -band observations - 2451200.0

Table 3. Velocity measurements for OGLEGC17

Number	# of spectra ^a	ϕ	$\Delta\phi$	V_1	$\sigma(V_1)$	V_2	$\sigma(V_1)$
1	3	0.001	0.078	232.9	9.7	232.9	9.7
2	5	0.142	0.030	305.8	15.4	167.7	20.7
3	5	0.176	0.035	308.5	10.6	141.0	13.2
4	4	0.206	0.022	317.5	16.2	140.5	9.8
5	4	0.233	0.021	314.0	10.2	142.2	19.4
6	6	0.346	0.067	309.6	8.3	169.2	13.2
7	4	0.562	0.031	213.8	6.1	260.7	11.3
8	2	0.768	0.014	145.3	9.3	323.6	14.2
9	5	0.795	0.073	170.8	11.6	332.7	10.7
10	5	0.039	0.042	283.5	13.9	233.6	15.2
11	4	0.085	0.031	276.9	14.2	216.4	15.5
12	6	0.247	0.056	314.0	14.6	134.3	10.9
13	7	0.826	0.066	160.4	8.3	332.3	12.3

^aNumber of spectra averaged

Table 4. Elements for OGLEGC17

Element	Value
P (days)	$2.4669384 \pm 0.0000023^a$
T_0 (HJD)	$2449082.3530 \pm 0.0008^a$
K_1 (km s $^{-1}$)	82.65 ± 3.25
K_2 (km s $^{-1}$)	97.04 ± 3.89
γ (km s $^{-1}$)	237.97 ± 1.93
e	0.0^b
m_2/m_1	0.852 ± 0.073

^aPhotometric ephemeris

^bAssumed value

Table 5. Photometric solutions of *BVI* light curves of OGLEGC17

parameter	Mode 0	Mode 2
i	87.162 ± 1.98	86.31 ± 1.04
Ω_1	5.645 ± 0.171	5.562 ± 0.063
Ω_2	9.745 ± 0.337	9.523 ± 0.133
T_1	5676*	5676*
T_2	6085*	6077 ± 40
$(l1/(l1 + l2))_B$	0.7597 ± 0.0029	0.7608 ± 0.0081
$(l1/(l1 + l2))_V$	0.7725 ± 0.0028	0.7694 ± 0.0078
$(l1/(l1 + l2))_I$	0.7811 ± 0.0039	0.7855 ± 0.0111
$(l2/(l1 + l2))_B$	0.2403 ± 0.0034	-
$(l2/(l1 + l2))_V$	0.2275 ± 0.0033	-
$(l2/(l1 + l2))_I$	0.2189 ± 0.0053	-
r_1 (pole)	0.2079 ± 0.0073	0.2114 ± 0.0028
r_1 (point)	0.2125 ± 0.0080	0.2166 ± 0.0031
r_1 (side)	0.2096 ± 0.0076	0.2133 ± 0.0029
r_1 (back)	0.2119 ± 0.0079	0.2157 ± 0.0031
r_2 (pole)	0.0982 ± 0.0038	0.1007 ± 0.0016
r_2 (point)	0.0984 ± 0.0038	0.1010 ± 0.0016
r_2 (side)	0.0983 ± 0.0038	0.1009 ± 0.0016
r_2 (back)	0.0984 ± 0.0038	0.1010 ± 0.0016
$\langle r_1 \rangle$	0.2105 ± 0.0077	0.2142 ± 0.0030
$\langle r_2 \rangle$	0.0983 ± 0.0038	0.1009 ± 0.0016

*not adjusted

Table 6. Absolute parameters for OGLEGC17

Element	Value
$A (R_{\odot})$	8.782 ± 0.248
$R_1 (R_{\odot})$	1.882 ± 0.059
$R_2 (R_{\odot})$	0.886 ± 0.029
$M_1 (M_{\odot})$	0.806 ± 0.056
$M_2 (M_{\odot})$	0.686 ± 0.047

Table 7. T_{eff} and L_{bol} for components of OGLEGC17

[Fe/H]	color	T_{eff_1}	T_{eff_2}	L_1/L_\odot	L_2/L_\odot
-1.74	$B - V$	5676 ± 176	6074 ± 192	3.30 ± 0.46	0.96 ± 0.14
-1.33	$B - V$	5739 ± 176	6141 ± 192	3.44 ± 0.47	1.00 ± 0.14
-1.74	$V - K$	5948 ± 44	6341 ± 47	3.97 ± 0.28	1.14 ± 0.08
-1.33	$V - K$	5926 ± 44	6322 ± 47	3.92 ± 0.27	1.12 ± 0.08

Table 8. Absolute visual magnitudes and distance moduli for components of OGLEGC17 quadrature

$[Fe/H]$	color	M_{V1}	M_{V2}	$(m - M)_{V1}$	$(m - M)_{V2}$
-1.74	$B - V$	3.65 ± 0.16	4.96 ± 0.17	13.81 ± 0.16	13.76 ± 0.17
-1.33	$B - V$	3.56 ± 0.16	4.89 ± 0.17	13.90 ± 0.16	13.83 ± 0.17
-1.74	$V - K$	3.42 ± 0.09	4.77 ± 0.09	14.04 ± 0.09	13.95 ± 0.09
-1.33	$V - K$	3.42 ± 0.09	4.76 ± 0.09	14.04 ± 0.09	13.96 ± 0.09

Table 9. Coefficients for S_V - Color Relations

color	constant	linear	quadratic	<i>rms</i>
$V - I$	2.522	2.816	-0.228	0.072
$V - J$	2.545	2.073	-0.089	0.058
$V - H$	2.592	1.496	-0.022	0.028
$V - K$	2.563	1.493	-0.046	0.023

Table 10. Colors for OGLEGC17

color	Max	Primary	Secondary
$(V - J)_0$	0.999	1.017	0.844
$(V - H)_0$	1.336	1.369	1.163
$(V - K)_0$	1.350	1.400	1.167

Table 11. Surface Brightnesses and Distances for OGLEGC17

color	$S_{V,pri}$	$S_{V,sec}(pc)$	$d_{pri}(pc)$	$d_{sec}(pc)$	$(m - M)_{V,pri}$	$(m - M)_{V,sec}$
$(V - J)$	4.617	4.271	5352	5385	14.04	14.06
$(V - H)$	4.624	4.322	5333	5259	14.04	14.01
$(V - K)$	4.583	4.262	5435	5406	14.08	14.07